

Photocatalytic Water Splitting into H_2 and O_2 over Titanate Pyrochlores $Ln_2Ti_2O_7$ (Ln = Lanthanoid: Eu–Lu)

Masanobu Higashi,[1,2] Ryu Abe,[1,3] Hideki Sugihara,[1] and Kazunari Domen*[2]

[1]National Institute of Advanced Industrial Science and Technology (AIST), 1-1-1 Higashi, Tsukuba 305-8565

[2]Faculty of Engineering, The University of Tokyo, 7-3-1 Hongo, Bunkyo-ku, Tokyo 113-8656

[3]Catalysis Research Center, Hokkaido University, Sapporo 001-0021

Received January 11, 2008; E-mail: domen@chemsys.t.u-tokyo.ac.jp

A series of titanate pyrochlore $Ln_2Ti_2O_7$ (Ln = Eu–Lu) was prepared by a polymerized complex method and evaluated as a photocatalyst for water splitting reaction. All the $Ln_2Ti_2O_7$, except for $Tb_2Ti_2O_7$, demonstrated evolution of H_2 and O_2 in a stoichiometric ratio from pure water under UV-light irradiation. The photocatalytic activities of the $Ln_2Ti_2O_7$ were significantly enhanced by the addition of excess Ln (5%) in the preparation procedure. As for the $Ln_2Ti_2O_7$ containing small Ln^{3+} (Ln = Dy–Lu), the enhanced photocatalytic activity can be explained by the suppression of impurity phase formation, rutile titanium oxide (TiO_2), which formed in the stoichiometric preparation at high temperature. It was also found that the addition of excess Ln increased the surface area of these materials, which certainly contributed to the enhanced photocatalytic activity. In the case of $Gd_2Ti_2O_7$, the photocatalytic activity was remarkably improved by the addition of excess Gd, in spite of the fact that no impurity phase formed even in the stoichiometric preparation. Scanning electron microscopy (SEM) and pore size distribution analysis revealed that the addition of excess amount of Gd made the $Gd_2Ti_2O_7$ material porous, which is undoubtedly one of the major factors enhancing the photocatalytic activity.

Photocatalytic water splitting into H_2 and O_2 by semiconductors has received much attention, because of its potential for production of clean fuel, H_2, from water utilizing solar light. Since the report of photoelectrochemical water splitting on TiO_2 photoelectrode by Honda and Fujishima, numerous efforts have been made to develop new photocatalyst materials.[1] Various mixed oxide materials have been so far reported to show reasonable activity for stoichiometric water splitting into H_2 and O_2 under UV light. However, most of the active materials are classified as perovskite compounds, e.g. $SrTiO_3$,[2–4] $K_2La_2Ti_3O_{10}$,[5] $ATaO_3$ (A = Li, Na, K, and Ag),[6–9] $Sr_2M_2O_7$ (M = Nb and Ta),[10] $RbNbTa_2O_7$,[11] $A_5M_4O_{15}$ (A = Sr and Ba, M = Nb and Ta),[12–14] and $La_2Ti_2O_7$.[15] Although pyrochlore structure, represented by the empirical formula $A_2B_2O_7$, is one of the biggest family of mixed oxide compounds, only a few studies have been made on application of the pyrochlore compounds as a semiconductor photocatalyst. We have recently reported an yttrium titanate, $Y_2Ti_2O_7$, as a first example of active pyrochlore compound for water splitting under UV-light irradiation.[16] The $Y_2Ti_2O_7$ samples prepared by a polymerized complex (PC) method, especially those prepared with excess amount (5%) of Y, showed much higher activity than that prepared by conventional solid-state reaction.[17] The excess amount of Y added was found to prevent the formation of impurity TiO_2 rutile, which forms at high temperature on the surface of $Y_2Ti_2O_7$ and decreases the photocatalytic activity. The optimum photocatalytic activity of $Y_2Ti_2O_7$ for water splitting was comparable to that of perovskite type semiconductor photocatalysts, suggesting that pyrochlore compounds are a potential candidate for efficient semiconductor materials to split water.

In the present study, a series of pyrochlore compounds $Ln_2Ti_2O_7$ (Ln = Eu–Lu) was prepared using PC method and their photocatalytic activity was evaluated for water splittng reaction under UV light. It was a mistake to think that $Ln_2Ti_2O_7$ photocatalysts with partly filled 4f orbitals (Ln = Eu–Yb) showed low activity.[16] Almost all $Ln_2Ti_2O_7$ photocatalysts containing 4f electrons split water into H_2 and O_2, irrespective of 4f electrons. It was found that the addition of excess Ln in the preparation procedure improved, more or less, the activity in a similar manner as $Y_2Ti_2O_7$, except for the case of $Eu_2Ti_2O_7$ and $Tb_2Ti_2O_7$. The change in photocatalytic activity is discussed from the viewpoint of ionic radius of Ln.

Experimental

Preparation. Powdered $Ln_2Ti_2O_7$ samples were prepared by the polymerized complex (PC) method.[18] First, 0.01 mol of titanium isopropoxide ($Ti[OCH(CH_3)_2]_4$) was dissolved in 0.4 mol of ethylene glycol (EG). Subsequently, 0.3 mol of anhydrous citric acid (CA) was added to the solution with continuous stirring. After complete dissolution of the CA, 0.01 mol (stoichiometric ratio of Ln and Ti) or 0.0105 mol (excess amount (5%) of Ln to Ti) of $Ln(NO_3)_3 \cdot nH_2O$ (or $LnCl_3 \cdot nH_2O$) was added. The mixture was magnetically stirred for 1 h to produce a colorless solution. The solution was heated to ca. 130 °C to accelerate esterification reactions between CA and EG and precipitate a transparent glassy resin. The resin was fired in an electric furnace for 2 h at 360 °C. The resulting black solid mass was ground into a powder and calcined on an Al_2O_3 plate at 800–1200 °C for 2 h in air. The $Ln_2Ti_2O_7$ samples prepared with excess amount (5%) of Ln to Ti are referred to as $Ln_2Ti_2O_7$-e, while those prepared with a

Published on the web October 10, 2008; doi:10.1246/bcsj.81.1315

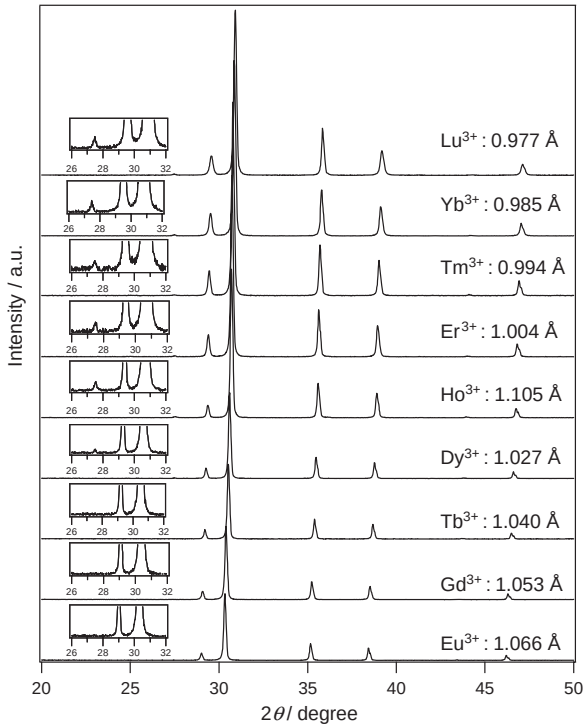

Figure 1. XRD patterns of $Ln_2Ti_2O_7$ (Ln = Eu–Lu) samples prepared with a stoichiometric ratio followed by calcination at 1000 °C for 2 h in air.

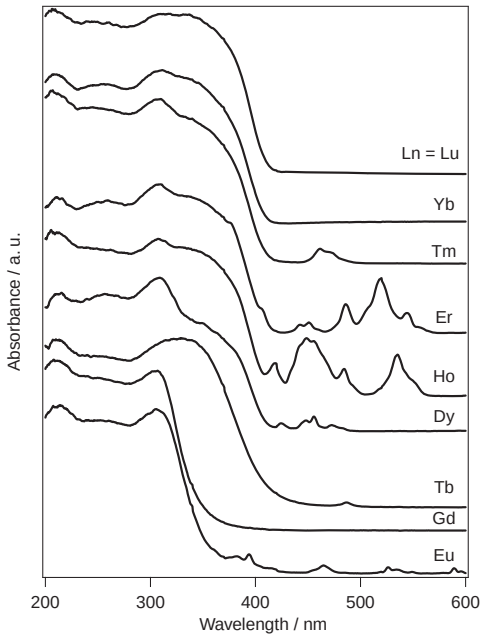

Figure 2. UV–vis DR spectra of $Ln_2Ti_2O_7$ (Ln = Eu–Lu) samples prepared with a stoichiometric ratio followed by calcination at 1000 °C for 2 h in air.

stoichiometric ratio of Ln and Ti are referred to as $Ln_2Ti_2O_7$-s.

Photocatalytic Reaction. NiO_x co-catalyst was loaded on the photocatalyst powder to promote H_2 production.[4] The photocatalyst powder prepared by the PC method was immersed into an aqueous solution containing the required amount of $Ni(NO_3)_2$. The solution was then evaporated to a dry solid using a water bath, followed by heating in air at ca. 300 °C for 20 min. The NiO_x-supported photocatalyst was then reduced in flowing H_2 at 500 °C for 2 h and subsequently oxidized at 200 °C for 1 h in air, in order to get NiO_x-supported photocatalyst. The photocatalytic reaction was examined using a gas closed circulation system. The photocatalyst powder (0.5 g) was suspended in distilled water (400 mL) by a magnetic stirrer in an inner-irradiation reaction cell. The light source (400-W high-pressure mercury lamp, Riko Kagaku Japan) was covered with a water jacket (quartz glass; cutoff $\lambda < 200$ nm) to keep the reactor temperature constant at 20 °C by cooling water. The gases evolved were analyzed by on-line gas chromatography (TCD, molecular sieve 5A) connected to the circulation system.

Characterization. The synthesized materials were studied by powder X-ray diffraction (MAC science, MX Lab.), scanning electron microscopy (SEM; Hitachi S-4700), and UV–visible diffuse reflectance spectroscopy (DRS; Jasco V-570). The Brunauer–Emmett–Teller (BET) surface area was measured with a Coulter SA-3100 instrument at liquid nitrogen temperature.

Results and Discussion

XRD Patterns and UV–Vis DR Spectra of the $Ln_2Ti_2O_7$ Prepared with Stoichiometric Ratio or with Excess Amount of Ln. Figure 1 shows XRD patterns of $Ln_2Ti_2O_7$-s samples prepared in stoichiometric ratio (Ln:Ti = 1:1) using the PC method followed by calcination at 1000 °C for 2 h in air. The XRD patterns of all $Ln_2Ti_2O_7$-s samples indicated a cubic-pyrochlore structure, in which the 2θ value of main peaks shifted toward lower angle with the increasing ionic radius of Ln^{3+}, from Lu^{3+} (six-coordination: 0.861 Å, eight-coordination: 0.977 Å) to Eu^{3+} (six-coordination: 0.947 Å, eight-coordination: 1.066 Å), indicating the increasing lattice constant of pyrochlore crystal structure with the increase in the size of Ln, as reported.[19] However, the XRD patterns of $Ln_2Ti_2O_7$-s with small Ln^{3+} (Ln = Dy–Lu) were found to contain impurity peaks assignable to titanium oxide (TiO_2) with rutile crystal phase at around $2\theta = 27.5°$, as shown in Figure 1. On the other hand, those of $Ln_2Ti_2O_7$-s with large Ln^{3+} (Ln = Tb, Gd, and Eu) indicated the formation of pure cubic pyrochlore phase, without formation of any impurity phases. Figure 2 shows UV–vis DR spectra of the $Ln_2Ti_2O_7$-s samples prepared by calcination at 1000 °C for 2 h in air. Although absorption peaks derived from f–f transition were observed on some $Ln_2Ti_2O_7$ samples in the visible light region, the main absorption of $Ln_2Ti_2O_7$-s exists in UV region shorter than 410 nm. The absorption edges of $Ln_2Ti_2O_7$-s samples with small Ln^{3+} (Ln = Dy–Lu) and $Tb_2Ti_2O_7$-s sample were observed at around 410 nm, while those of $Ln_2Ti_2O_7$-s samples with large Ln^{3+} (Ln = Gd and Eu) exist at around 350 nm. Judging from the fact that the TiO_2 rutile impurity phase was observed in the XRD patterns of $Ln_2Ti_2O_7$-s containing small Ln (Ln = Dy–Lu), it is speculated that the absorption longer than 350 nm observed in the $Ln_2Ti_2O_7$-s (Ln = Dy–Lu) is derived from the TiO_2 rutile, which has an absorption edge at 410 nm. We have previously reported that such formation of TiO_2 rutile phase occurred in $Y_2Ti_2O_7$ samples prepared with stoichiometric ratio (Y:Ti = 1:1) by PC method, and it was effectively prevented by the addition of excess amount of Y in the synthesis procedure.[17] Then, the addition of excess Ln was attempted to suppress the formation of impurity TiO_2 rutile phase in the same way.

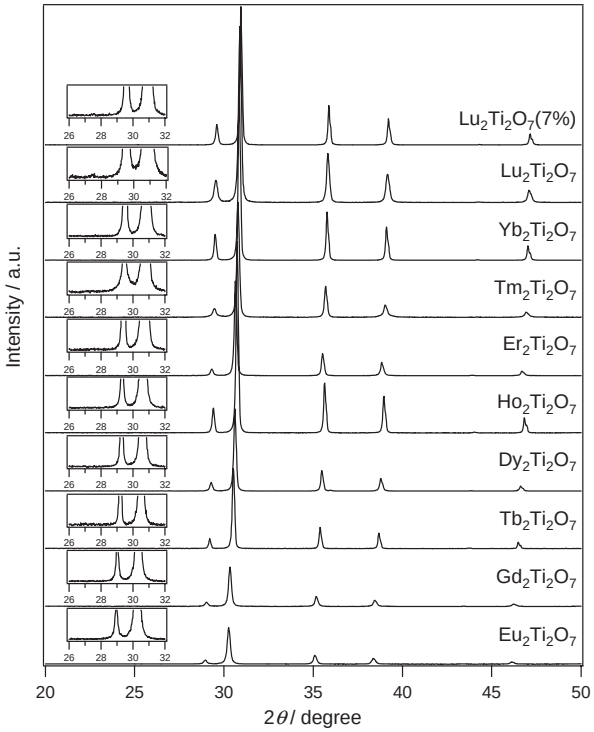

Figure 3. XRD patterns of $Ln_2Ti_2O_7$ (Ln = Eu–Lu) samples prepared with excess amount of Ln (5%) followed by calcination at 1000 °C for 2 h in air.

Figure 3 shows the XRD patterns of $Ln_2Ti_2O_7$-e samples prepared with excess amount of Ln (Ln:Ti = 1.05:1) and followed by calcination at 1000 °C. Except for $Lu_2Ti_2O_7$, all diffraction peaks can be assigned to pure pyrochlore structure; no peak assignable to impurities such as TiO_2 and Ln_2O_3 was observed. With the disappearance of peaks attributable to TiO_2 impurity in XRD patterns, the absorption from 350 to 410 nm, which was observed in the sample prepared in stoichiometric ratio, vanished in the UV–vis DR spectra of $Ln_2Ti_2O_7$-e (Ln = Dy–Yb) samples, as shown in Figure 4. This indicates that the absorption from 350 to 410 nm originated from the TiO_2 rutile impurity, not from pyrochlores themselves. As for the $Lu_2Ti_2O_7$-e sample, the formation of TiO_2 rutile was successfully prevented by the addition of further excess Lu (7%), while the sample prepared with 5% excess of Lu still contained a small amount of TiO_2 rutile. In the case of $Tb_2Ti_2O_7$, the sample prepared in a stoichiometric ratio, $Tb_2Ti_2O_7$-s, has an absorption edge at around 410 nm regardless of the absence of impurity TiO_2 phase in XRD, and the addition of excess Tb resulted in broad absorption in the visible light region up to 600 nm. Although the origin of these absorptions is not clear at the present, the phenomena observed for $Tb_2Ti_2O_7$ was apparently different from other $Ln_2Ti_2O_7$ materials and this might be a reason for the inactiveness of $Tb_2Ti_2O_7$ for photocatalytic water splitting, as described in the next section.

In summary, it was found that the TiO_2 rutile impurity phase tends to form in $Ln_2Ti_2O_7$ containing small Ln, from Lu (six-coordination: 0.861 Å, eight-coordination: 0.977 Å) to Dy (six-coordination: 0.912 Å, eight-coordination: 1.027 Å), when they were prepared in a stoichiometric ratio (Ti:Ln =

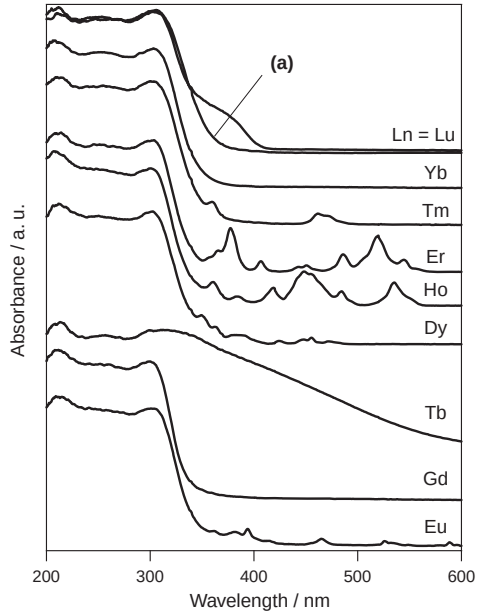

Figure 4. UV–vis DR spectra of $Ln_2Ti_2O_7$ (Ln = Eu–Lu) samples prepared with excess amount of Ln (5%) followed by calcination at 1000 °C for 2 h in air. (a): $Lu_2Ti_2O_7$ prepared with excess amount of Lu (7%).

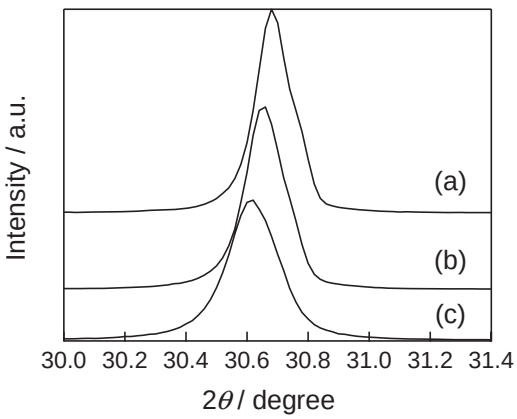

Figure 5. XRD patterns (main peaks) of $Y_2Ti_2O_7$ samples prepared with (a) a stoichiometric ratio followed by calcination at 1200 °C for 24 h using solid-state reaction, (b) a stoichiometric ratio followed by calcination at 1000 °C for 2 h using polymerized complex method, and (c) excess amount of Y (5%) followed by calcination at 1000 °C for 2 h using polymerized complex method.

1:1). On the other hand, a pure pyrochlore phase of $Ln_2Ti_2O_7$ was obtained with large Ln (Ln = Eu, Gd, and Tb) even by the stoichiometric preparation, while $Tb_2Ti_2O_7$ sample exhibited different character from others in the UV–vis spectrum. The formation of TiO_2 rutile in the $Ln_2Ti_2O_7$-s with small Ln^{3+} (Ln = Dy–Lu) is possibly explained by the partial replacement of Ti^{4+} (six-coordination: 0.605 Å) in B sites of $A_2B_2O_7$ by Ln^{3+} or invasion of interstitial space in $Ln_2Ti_2O_7$ by Ln^{3+}, which causes a surplus of Ti atoms and resulting in the TiO_2 rutile formation after the calcination. Excess amount of Ln^{3+} probably invaded interstitial space in $Ln_2Ti_2O_7$. These results were supported by XRD measurement. As shown in Figure 5

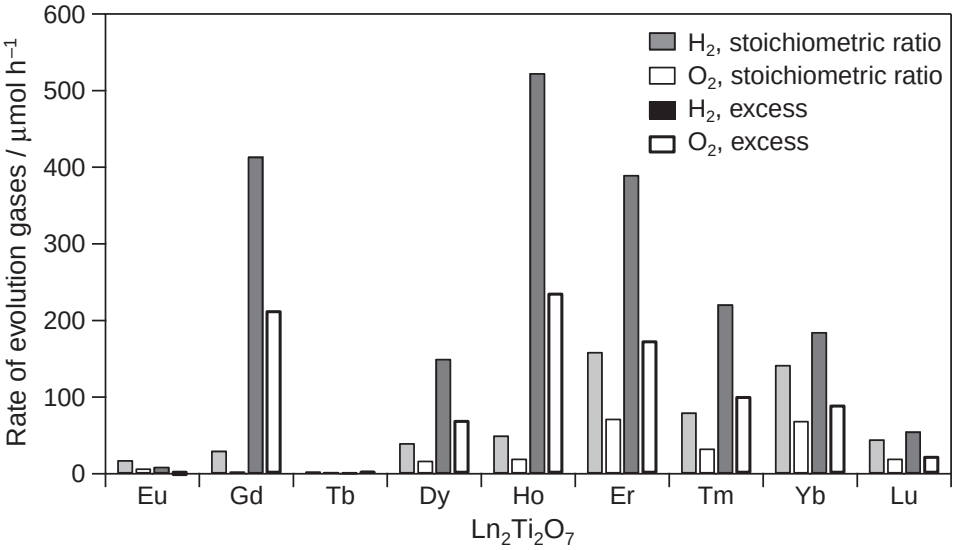

Figure 6. Rates of H_2 and O_2 evolution over 1 wt % NiO_x–$Ln_2Ti_2O_7$ (Ln = Eu–Lu) prepared with stoichiometric ratio and excess amount of Ln (5%) (Lu: 7%).

($Y_2Ti_2O_7$, for example), the main peak was shifted to lower angles (2θ) with increasing amount of Y invasion. The addition of excess amount of Ln was found to effectively prevent the TiO_2 rutile formation, and resulted in the production of pure $Ln_2Ti_2O_7$ samples in all case. It should be noted here that the addition of excess amount of Ln caused no negative effect, such as formation of Ln_2O_3 impurity phase.

Photocatalytic Activities of the $Ln_2Ti_2O_7$ (Ln = Dy–Lu) Containing Ln^{3+} with Small Ionic Radius. Figure 6 summarize the rates of H_2 and O_2 evolution over NiO_x (1 wt %)–$Ln_2Ti_2O_7$-s and NiO_x (1 wt %)–$Ln_2Ti_2O_7$-e samples irradiated with UV light in pure water. All the samples shown in Figure 6 were prepared by calcination at 1000 °C for 2 h. It was found that all the $Ln_2Ti_2O_7$ samples, except for $Tb_2Ti_2O_7$, exhibited activity for overall water splitting into H_2 and O_2. As for the $Ln_2Ti_2O_7$ containing small Ln^{3+} (Ln = Dy–Lu), it was confirmed that the addition of excess amount of Ln obviously improved the photocatalytic activity of all the samples. For example, the rate of gas evolution over $Ho_2Ti_2O_7$-e was ca. 10 times higher than that over the $Ho_2Ti_2O_7$-s. The improved photocatalytic activity of $Ln_2Ti_2O_7$ (Ln = Lu–Dy) with the excess Ln addition can be well explained by the suppression of TiO_2 rutile impurity phase, which formed at high temperature and decrease the photocatalytic activity of $Ln_2Ti_2O_7$. As an example, the rates of H_2 evolution over the NiO_x–$Dy_2Ti_2O_7$-s and NiO_x–$Dy_2Ti_2O_7$-e samples are plotted as a function of calcination temperature in Figure 7a, wherein data for specific surface area of each sample are also shown (the rate of O_2 evolution was omitted). The rate of H_2 evolution over NiO_x–$Dy_2Ti_2O_7$-e, which was prepared with an excess amount of Dy, significantly increased with the increase of calcination temperature from 800 to 1100 °C, and decreased at 1200 °C. The surface area of $Dy_2Ti_2O_7$-e drastically decreased with the increase of calcination temperature from 800 to 1100 °C. In this temperature range, no TiO_2 rutile phase was observed in the XRD patterns of $Dy_2Ti_2O_7$-e samples (as shown in Figure 3), indicating the formation of pure pyrochlore $Dy_2Ti_2O_7$ phase when they ware prepared with an

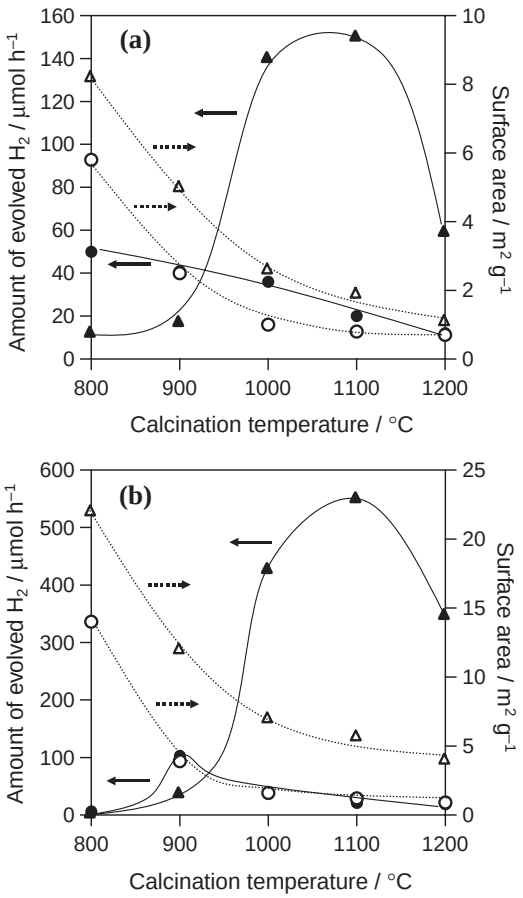

Figure 7. The rates of H_2 evolution (closed circle) and specific surface areas (open circle) of 1 wt % NiO_x–(a) $Dy_2Ti_2O_7$-s (or (b) $Gd_2Ti_2O_7$-s) and the rates of H_2 evolution (closed triangle) and specific surface area (open triangle) of 1 wt % NiO_x–(a) $Dy_2Ti_2O_7$-e (or (b) $Gd_2Ti_2O_7$-e) as a function of calcination temperature.

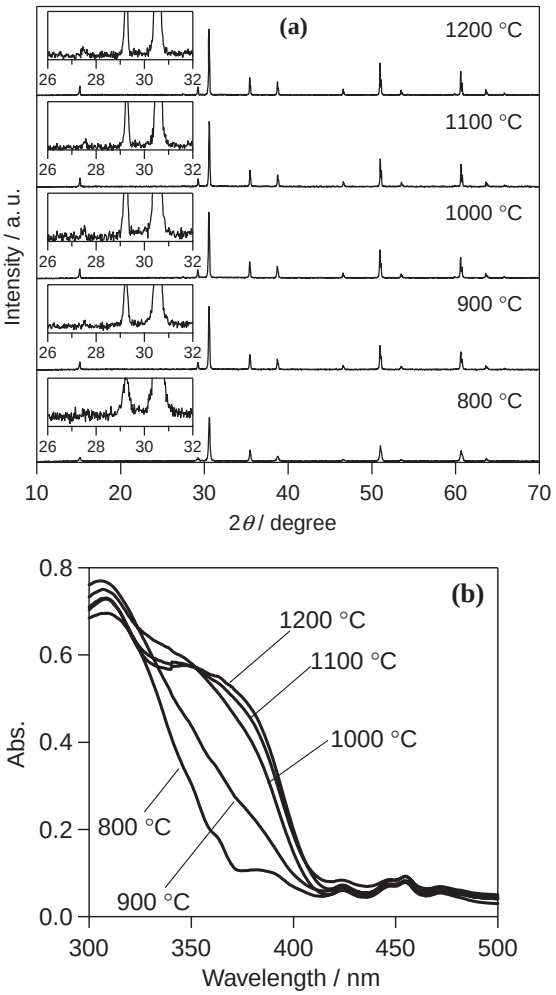

Figure 8. (a) XRD patterns and (b) UV–vis DR spectra of $Dy_2Ti_2O_7$ prepared with stoichiometric ratio followed by calcination at 800–1200 °C for 2 h.

excess amount of Dy. Therefore, the increase of photocatalytic activity of $Dy_2Ti_2O_7$-e from 800 to 1100 °C is almost certainly due to the increase in crystallinity of the $Dy_2Ti_2O_7$ material. On the other hand, the rates of H_2 evolution over $Dy_2Ti_2O_7$-s samples, which ware prepared in a stoichiometric ratio, monotonically decreased with the increase of calcination temperature, in spite of the increasing crystallinity indicated by the decrease in the surface area. As shown in XRD patterns and UV–vis spectra (Figure 8), the $Dy_2Ti_2O_7$-s samples calcined above 900 °C contained the impurity phase of TiO_2 rutile. It has been revealed that the TiO_2 rutile powder photocatalyst itself has no ability to split pure water into H_2 and O_2. As shown in Figure 2, the $Dy_2Ti_2O_7$ sample calcined at 1000 °C possesses a strong absorption at wavelengths longer than 350 nm, which is undoubtedly due to the TiO_2 impurity phase, in spite of the small amount TiO_2 rutile phase indicated by the weak peaks observed in the XRD pattern. This indicates that the TiO_2 rutile phase formed mainly on the surface of $Dy_2Ti_2O_7$. Therefore, we can conclude that the TiO_2 rutile phase which has no ability to split water into H_2 and O_2 formed on the outer surface of $Dy_2Ti_2O_7$-s particles and deactivated the active site of $Dy_2Ti_2O_7$ material prepared above 900 °C, resulting in low

Table 1. BET Surface Area of $Ln_2Ti_2O_7$ (Ln = Eu–Lu) Samples Calcined at 1000 °C for 2 h

Photocatalyst	Surface area/$m^2\ g^{-1}$	
	Stoichiometric ratio	5% excess
$Lu_2Ti_2O_7$	0.9	2.0
$Yb_2Ti_2O_7$	0.9	1.9
$Tm_2Ti_2O_7$	0.7	2.4
$Er_2Ti_2O_7$	0.8	2.1
$Ho_2Ti_2O_7$	0.9	2.0
$Dy_2Ti_2O_7$	1.1	2.6
$Tb_2Ti_2O_7$	1.0	2.6
$Gd_2Ti_2O_7$	1.6	5.7
$Eu_2Ti_2O_7$	1.6	6.9

photocatalytic activities, while the $Dy_2Ti_2O_7$ material inside might have potential activity. No TiO_2 rutile particle was observed by SEM. We also found that the addition of an excess amount of Ln increase the surface areas of the materials as clearly seen in Figure 7a, in which all the surface areas of $Dy_2Ti_2O_7$-e samples were higher than those of $Dy_2Ti_2O_7$-s samples at each calcination temperature. The increase in surface area was observed for the all $Ln_2Ti_2O_7$ samples by addition of excess Ln, as shown in Table 1. The addition of excess Ln probably suppresses crystal growth, resulting in increase of surface area. Therefore, it is strongly suggested that the increase in surface area is another significant reason for the increased photocatalytic activity of $Ln_2Ti_2O_7$-e compared to $Ln_2Ti_2O_7$-s samples, as well as the suppression of TiO_2 impurity formation at high temperature.

From the point of view of $Ln_2Ti_2O_7$-e containing small Ln^{3+}, the photocatalytic activity increased from Lu to Ho, and decreased to Dy. $Ho_2Ti_2O_7$-e photocatalyst has high activity in the $Ln_2Ti_2O_7$-e with small Ln^{3+}. The ionic radius of Ho^{3+} (eight-coordination: 1.015 Å) is quite near to that of Y^{3+} (eight-coordination: 1.019 Å) in $Y_2Ti_2O_7$ that shows the highest activity[17] of all $Ln_2Ti_2O_7$ pyrochlores, possibly implying that photocatalytic activity is influenced by ionic radius of Ln^{3+}.

Photocatalytic Activities of the $Ln_2Ti_2O_7$ (Ln = Eu–Tb) Containing Ln^{3+} with Large Ionic Radius. As for the $Gd_2Ti_2O_7$ samples, the photocatalytic activity drastically increased by the addition of an excess amount of Gd as shown in Figure 6, regardless of the fact that no TiO_2 impurity phase was formed even when they were prepared with stoichiometric ratio at 1000 °C (Figure 1). This implies the presence of other factors that increase the photocatalytic activity. Figure 7b shows the relationship of the rate of H_2 gas evolution over $Gd_2Ti_2O_7$ samples with their calcination temperature. Contrary to the results on $Dy_2Ti_2O_7$ (Figure 7a), the photocatalytic activity of $Gd_2Ti_2O_7$-s samples prepared with a stoichiometric ratio increased with increase of calcination temperature from 800 to 900 °C, certainly due to the increased crystallinity, and decreased above 1000 °C. As described previously, no TiO_2 impurity phase was observed for $Gd_2Ti_2O_7$-s samples throughout this calcination temperature range from 800 to 1200 °C. Therefore, it is suggested that the intrinsic property of $Gd_2Ti_2O_7$ material itself was observed without suffering from TiO_2 impurity phase. That is, the photocatalytic activity initially increased with increase of calcination temperature due

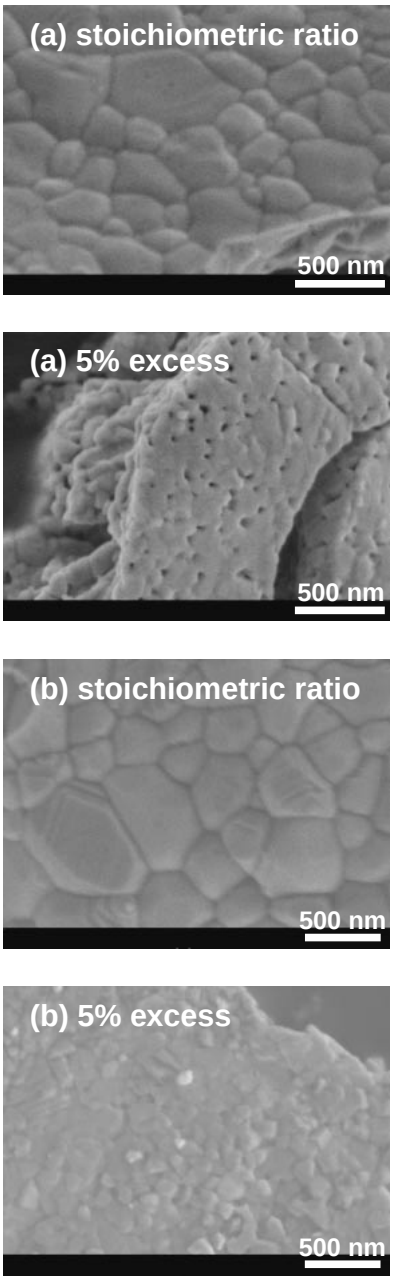

Figure 9. SEM images of (a) $Gd_2Ti_2O_7$ and (b) $Dy_2Ti_2O_7$ samples prepared with stoichiometric ratio and excess amount of Gd (or Dy) (5%).

to crystallization, and then decreased at higher temperature ascribing to the decrease in the surface area of materials. With the addition of excess amount of Gd, the rate of H_2 evolution drastically improved with the increase of calcination temperature from 800 to 1100 °C, similar to the case of $Dy_2Ti_2O_7$ samples. As shown in Table 1, the surface area of $Gd_2Ti_2O_7$-e prepared at 1000 °C is higher than those of $Ln_2Ti_2O_7$-e samples containing small Ln (Ln = Lu–Tb). Figure 9a shows SEM images of $Gd_2Ti_2O_7$-s and $Gd_2Ti_2O_7$-e samples calcined at 1000 °C. Primary particle size of $Gd_2Ti_2O_7$-s and $Gd_2Ti_2O_7$-e are ca. 200–500 and 50–150 nm, respectively. It is clearly observed that the $Gd_2Ti_2O_7$-e samples have many pores with diameter of 20 to 50 nm, while the $Gd_2Ti_2O_7$-s sample

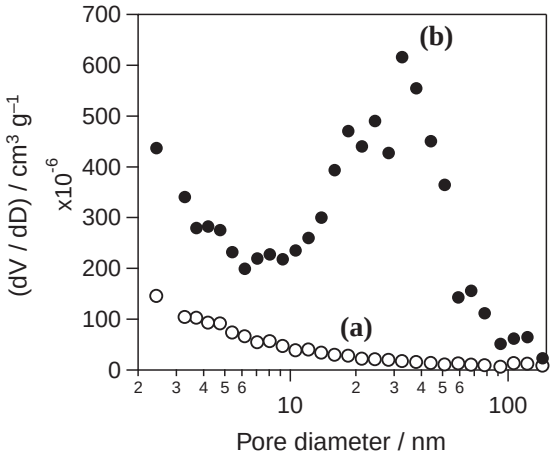

Figure 10. Pore-size distribution of $Gd_2Ti_2O_7$ prepared with (a) stoichiometric ratio and (b) excess amount of Gd (5%).

possesses flat surface. Figure 10 shows the pore-size distribution of $Gd_2Ti_2O_7$-s and $Gd_2Ti_2O_7$-e samples. The estimated diameter of channels inside the $Gd_2Ti_2O_7$-e sample, which were observed as holes on its surface in the SEM image, has in fact a size distribution between 20 to 50 nm. Such pores were not found in other $Ln_2Ti_2O_7$-e samples containing small Ln (Ln = Lu–Dy) even when they were calcined at high temperature above 1000 °C (The SEM image of $Dy_2Ti_2O_7$ samples are shown in Figure 9b, for example. Primary particle size of $Dy_2Ti_2O_7$-s and $Dy_2Ti_2O_7$-e are ca. 300–800 and 100–200 nm, respectively.). The formation of pore channels may be attributed to aggregation of $Gd_2Ti_2O_7$-e particles, which are smaller than other $Ln_2Ti_2O_7$ containing small Ln^{3+} particles. The depth of pore channels would be ca. 100–300 nm due to disordered aggregation of $Gd_2Ti_2O_7$-e particles. From these results, we can therefore conclude that formation of pore channels is another reason for the improved photocatalytic activity of $Gd_2Ti_2O_7$ material prepared with excess amount of Gd. The pore channels probably provided a short distance for the excited electrons and holes to migrate to the surface. Such a formation of pores was also observed in $Eu_2Ti_2O_7$-e, which contains the largest Eu^{3+} cation among the Ln^{3+} cations investigated in the present study, and actually the $Eu_2Ti_2O_7$-e had the highest surface area among the $Ln_2Ti_2O_7$ samples, as shown in Table 1. However, the photocatalytic activities of $Eu_2Ti_2O_7$ samples were negligibly low, regardless of their preparation procedure, as shown in Figure 6. The Eu^{3+} can trap the photogenerated electrons, because it can take a divalent oxidation number (Eu^{2+}). Such electron capture will suppress the supply of electrons to produce H_2, and also will act as recombination center by reacting with holes to reproduce Eu^{3+}, resulting in low photocatalytic activity. The $Tb_2Ti_2O_7$ material exhibited a unique photoabsorption property different from other $Ln_2Ti_2O_7$ materials, as shown in Figure 4. The broad absorption in visible region up to 600 nm probably results from Tb^{4+} in $Tb_2Ti_2O_7$ sample. Josse et al. have reported that the color of $Rb_2AlTb_3F_{16}$ and $RbAl_2Tb_4F_{22}$, containing both Tb^{3+} and Tb^{4+}, was red brown and orange, respectively.[20] Tb^{4+} also will act as a recombination center, as well as Eu^{2+}, resulting in low activity.

Conclusion

A series of titanate pyrochlore $Ln_2Ti_2O_7$ (Ln = lanthanoid: Eu–Lu) prepared by a polymerized complex method was first demonstrated to show photocatalytic activity for water splitting under UV light irradiation. It was found in the present study that the ratio of Ln to Ti in the preparation procedure significantly affects the photocatalytic activity of these materials, resulting from TiO_2 impurity formation, change in BET surface area, and change in morphologies. The appropriately synthesized $Ln_2Ti_2O_7$ materials have demonstrated relatively high photocatalytic activity for water splitting reaction, indicating the potential of these materials as an efficient photocatalyst for various reactions or as a base material for further modification such as doping.

References

1 A. Fujishima, K. Honda, *Nature* **1972**, *238*, 37.

2 K. Domen, S. Naito, M. Soma, T. Onishi, T. Tamaru, *J. Chem. Soc., Chem. Commun.* **1980**, 543.

3 J. Lehn, J. Sauvage, R. Ziessel, L. Halaire, *Isr. J. Chem.* **1982**, *22*, 168.

4 K. Domen, A. Kudo, T. Ohnishi, *J. Catal.* **1986**, *102*, 92.

5 T. Takata, K. Shinohara, A. Tanaka, M. Hara, J. N. Kondo, K. Domen, *J. Photochem. Photobiol., A* **1997**, *106*, 45.

6 H. Kato, A. Kudo, *J. Phys. Chem. B* **2001**, *105*, 4285.

7 H. Kato, H. Kobayashi, A. Kudo, *J. Phys. Chem. B* **2002**, *106*, 12441.

8 H. Kato, K. Asakura, A. Kudo, *J. Am. Chem. Soc.* **2003**, *125*, 3082.

9 T. Ishihara, H. Nishiguchi, K. Fukamachi, Y. Takita, *J. Phys. Chem. B* **1999**, *103*, 1.

10 A. Kudo, H. Kato, S. Nakagawa, *J. Phys. Chem. B* **2000**, *104*, 571.

11 M. Machida, J. Yabunaka, T. Kijima, *Chem. Mater.* **2000**, *12*, 812.

12 Y. Miseki, H. Kato, A. Kudo, *Chem. Lett.* **2006**, *34*, 1052.

13 H. Otsuka, K. Kim, A. Kouzu, I. Takimoto, H. Fujimori, Y. Sakata, H. Imamura, T. Matsumoto, K. Toda, *Chem. Lett.* **2005**, *34*, 822.

14 K. Yoshioka, V. Petrykin, M. Kakihana, H. Kato, A. Kudo, *J. Catal.* **2005**, *232*, 102.

15 D. W. Hwang, H. G. Kim, J. Kim, K. Y. Cha, Y. G. Kim, J. S. Lee, *J. Catal.* **2000**, *193*, 40.

16 R. Abe, M. Higashi, Z. Zou, K. Sayama, Y. Abe, *Chem. Lett.* **2004**, *33*, 954.

17 M. Higashi, R. Abe, Z. Zou, K. Syama, Y. Abe, *Chem. Lett.* **2005**, *34*, 1122.

18 M. Kakihana, M. M. Milanova, M. Arima, T. Okubo, M. Yashima, M. Yoshimura, *J. Am. Ceram. Soc.* **1996**, *79*, 1673.

19 O. Knop, F. Brisse, L. Castelliz, *Can. J. Chem.* **1969**, *47*, 971.

20 M. Josse, M. Dubois, M. El-Ghozzi, D. Avignant, *J. Alloys Compd.* **2004**, *374*, 213.